Malaysian Journal of Chemistry, 2026, Vol. 28(3), 212-223
(Special Issue: *International Conference on Chemistry and Sustainability, IC-CS 2025*)

Sol-Gel Synthesis of Metal Oxides and their Comparison

Neha Bhatt, Adeeba Mirza and Abhilasha Mishra*
Department of Chemistry, Graphic Era Deemed to be University, Dehradun, 248002, Uttarakhand, India
*Corresponding author (e-mail: abhi1680@gmail.com)

In this study, the preparation and characterization of nanosilica (SiO_2), nanotitania (TiO_2), nanoalumina (Al_2O_3), and nanozirconia (ZrO_2) sols via the sol-gel methodology using acid- and base-catalyzed reactions is discussed. Various precursors, tetraethoxyorthosilicate (TEOS), titanium isopropoxide (TTIP), aluminium nitrate nonahydrate, and zirconium (IV) isopropoxide, were hydrolyzed and condensed in optimized conditions with suitable catalysts and solvents. The prepared nano-sol solutions were analyzed using various techniques. The nano-dimensional characteristics of the sols were confirmed through particle size analysis, with average particle sizes and zeta potential values indicating high colloidal stability. The sols verified the Tyndall effect, signifying their colloidal nature. FTIR spectroscopy further confirmed the presence of functional groups and bonding structures specific to SiO_2, TiO_2, Al_2O_3, and ZrO_2 nanoparticles in the prepared sol solutions. Key features included Si-O-Si, Ti-O-Ti, Al-O, and Zr-O vibrations, indicative of their respective nanostructures. The successful synthesis and characterization of these stable nano-sols establish their potential for advanced applications, such as superhydrophobic coatings and other surface modifications.

Keywords: Tyndall effect, Particle Size Analysis, Zeta Potential, Colloidal Nature, Fourier Transform InfraRed Spectroscopy

Received: March 2026; Accepted: April 2026

Nano-particles are used in various products, from cosmetics to construction and science. Worldwide attention is received by sol-gel technology because of its versatility for synthesizing nanoparticles in an auspicious way. Controlled composition, unique and low cost, low-temperature processing of organic/ inorganic hybrid materials are the key features of this technology [1]. Nanotechnology is the technology that provides a material with improved and novel functionalities and characteristics. Because of their unique and different property from bulk material, Nanoparticles (NPs) are used enormously in different industries and in research [2]. There are two kinds of catalysis in sol-gel reactions: one is base catalysis, and the other is acid catalysis. The degree of deprotonation is lower in Acid-catalysed sols as compared to base-catalysed reaction; it's because in the base-catalyzed system, high branching is present.

Nano silica is known for its exclusive properties like high chemical inertness, low toxicity, and very high optical transparency; because of these properties, its application range and eligibility area have become very wide. SiO_2 nanoparticles have wide applications in thin films on solar panels, glass, and plastic for superhydrophobicity when combined with any modifier [1].

Titania shows a high refractive index (n = 2.4), so it is used in industries like pharmaceuticals, coatings, cosmetics, textiles, etc. Titania shows properties like self-cleaning and antifogging properties, due to which it is used for the preparation of anti-fogging car mirrors, window tiles, etc. Titania NPs have immense industrial applications and also serve as environment sanitizing agents, used for reducing the toxicity of products like dyes and drugs, treatment of wastewater, silkworm reproduction, space applications, etc. [2].

Alumina nanoparticles are one of the emerging application trends and can be created by many techniques like laser ablation, sol–gel, ball-milling, sputtering, etc., with interesting properties like low toxicity, low cost, high hardness, chemically stable, high thermal and mechanical stability, mechanical strength and stiffness, conductivity, high insulation and high optical transparency in the visible region. Nano alumina is inert towards acids and bases. Because of its unique characteristics, it is used in surface protective coatings, insulators, and the preparation of composite materials [3-4]. It has a high adsorption capacity. Aluminium oxide or alumina possesses a very strong bond between aluminium and oxygen, due to which it possesses high hardness and chemical stability. Therefore, it is widely used as a structural ceramic due to its wear resistance and corrosion resistance [5]. Nano-Alumina is also used for electrical insulation. It protects against abrasion on the coated surface. Its inertness and easy

†Paper presented at the International Conference on Chemistry and Sustainability, IC-CS 2025

biodegradability make it useful for implants. Because biodegradable behaviour is well accepted by the biological environment [4,6-7].

Nanoparticles like Silica is using in self-cleaning coatings [8], anti-icing [9], and for oil water separation [10], Titania nanoparticles can be used in photocatalytic self-cleaning surfaces [11], and UV protective coatings [1], Alumina nanoparticles are also using in oil-water separation [13], and for abrasion resistant [14], Zirconia particles using in thermal barrier coatings [15].

In this work, an easy laboratory development method of nano-sols of silica, titania, alumina, and zirconia was developed. As there are many existing methods to form nanoparticles. The easiest optimized method, the sol-gel methodology, is focused on in this paper and the prepared sol solution was analysed.

The novelty of this study lies in the synthesis of four distinct oxide-based nanoparticles (SiO_2, TiO_2, Al_2O_3, and ZrO_2) using a versatile and cost-effective sol-gel method. This comparative and multifunctional approach enables the evaluation and tailoring of surface and structural properties of each nanomaterial for specific industrial and environmental applications, including oil-water separation, self-cleaning, anti-corrosion, and thermal protection. Such synergistic modification strategies have rarely been explored systematically across this range of oxides, making the study both novel and impactful.

EXPERIMENTAL

Materials and Methods used to Prepare the Sol Solution

Tetraethoxyorthosilicate (TEOS), Titanium Tetra Isopropoxide (TTIP), Aluminium Nitrate Nonahydrate ($Al(NO_3)_3.9H_2O$), Zirconium (IV) Isopropoxide solution (70 wt% in 1 – propanol), Ammonium hydroxide (NH_4OH), Ethyl alcohol (EtOH), Hydrochloric acid (HCl), Glacial acetic acid (CH_3COOH), sodium hydroxide (NaOH). All Chemicals used were Laboratory-grade reagents.

Preparation of Sols

An optimized amount of precursor solution was taken, dissolved in an appropriate amount of solvent solution, and stirred for a few hours in the presence of acid or base. After keeping for a few days, hydrolysis and condensation reactions occurred. Nanosols of silica, titania, alumina, and zirconia were formed. Here is a detailed method for preparing nano titania, nano alumina, and nano zirconia sol as shown in Figure 1.

Preparation of Silica Sol

An optimized amount of tetraethoxysilane (TEOS), it's basically a silica precursor, which was used in the ratio of 1:1 with ethyl alcohol (EtOH) solvent. At a speed of 500 rpm, the solution was stirred continuously for 2 hours. To initialize reaction or catalyze the reaction, 1N ammonium hydroxide (NH_4OH) or 1M hydrochloric acid was added drop-wise. The whole reaction was carried out at room temperature for complete hydrolysis. After hydrolysis, the prepared solution was kept at dry place for four days to get a nano-dispersed silica sol [1].

Hydrolysis:

$$Si(OR)_4 + mH_2O \rightarrow Si(OR)_{4-n}(OH)_n + nROH$$

Condensation:

$$-Si-OH + RO-Si- \rightarrow -Si-O-Si- + R-OH$$

Poly-condensation:

$$n[-Si-OH] \rightarrow [-Si-O-Si-]_n + H_2O$$

Preparation of Titania Sol

The titania sol solution was prepared by an acid-catalysed reaction. The metal oxide precursor solution, which is used to prepare titania nano sol, is titanium isopropoxide (TTIP).

250 ml of water was taken in a conical flask, and then 15 ml of glacial acetic acid was added to it. 4 ml conc. HCl was added in the following manner. The solution was stirred on a magnetic stirrer at 60˚C. In the stirring solution, 15 ml of TTIP solution was added drop-wise. The solution was constantly stirred at 60 ˚C for 2.5 hours, then the solution was kept at room temperature for four days. This prepared solution was further analyzed if it is perfectly formed or not.

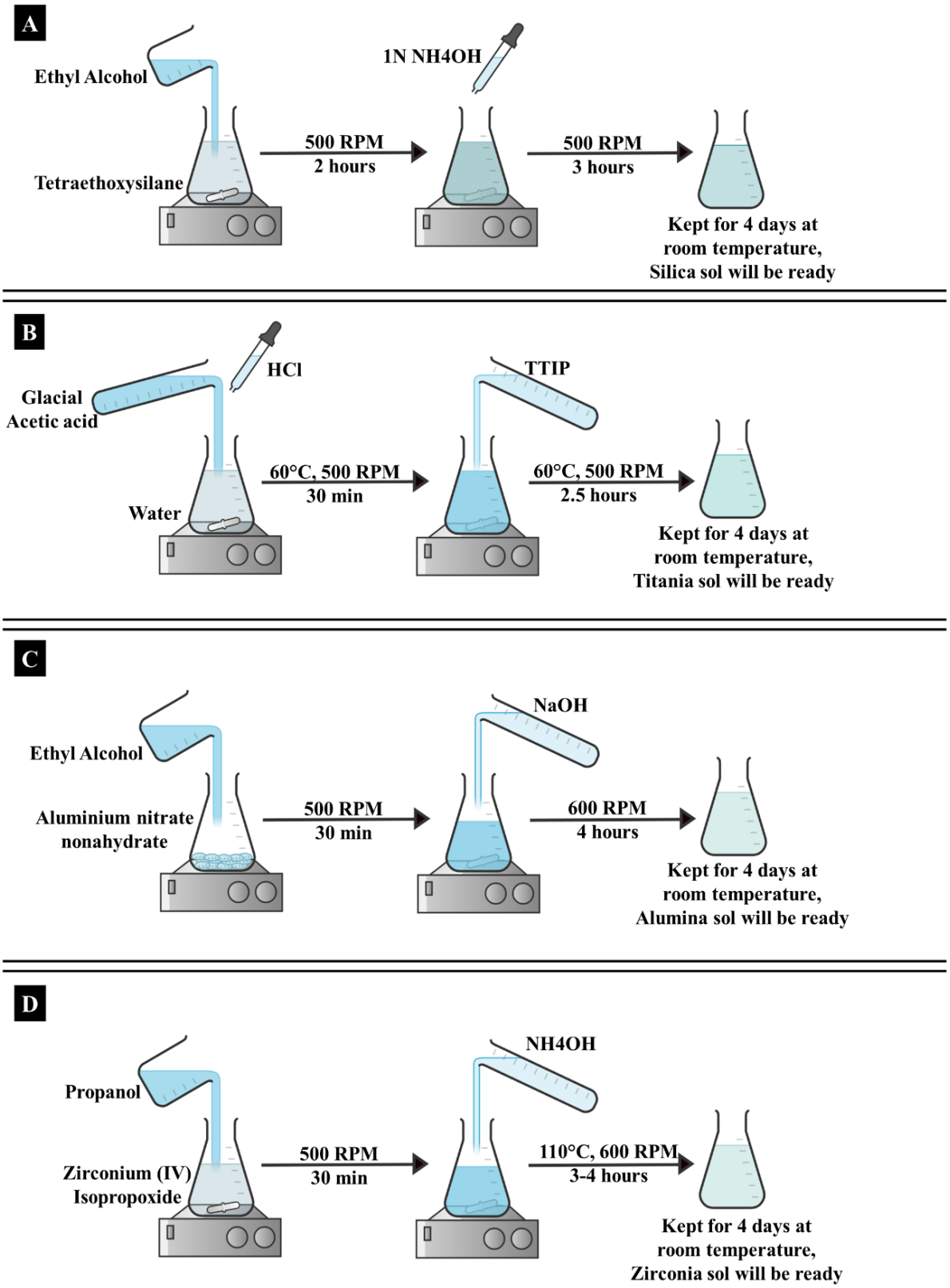

Figure 1. Process of (a) Silica sol, (b) Titania sol, (c) Alumina sol, (d) Zirconia sol.

Steps Involved in the Preparation of Titania Sol-

Hydrolysis

$$Ti(OR)_4 + mH_2O \rightarrow Ti(OR)_{4-n}(OH)_n + nROH$$

Condensation-

$$-Ti-OH + RO-Ti- \rightarrow -Ti-O-Ti- + R-OH$$

Titania sol

Poly-condensation-

$$-Ti-OH + HO-Ti- \rightarrow [-Ti-O-Ti-]_n + H_2O$$

Titania sol solution

Preparation of Alumina Sol

The following precursor, aluminium nitrate nonahydrate ($Al(NO_3)_3.9H_2O$), was used for the aluminium oxide (alumina) nano sol solution. 0.5 g aluminium nitrate nonahydrate salt was taken, and 50 ml of ethyl alcohol was added to it. By taking precursor, solvent, and 1N NaOH (for base catalysis) the sol was prepared with stirring at 600 rpm for 4 hours, then the solution was kept for four days for complete hydrolysis of reaction. The nano-sol solution was ready for further use and characterization [4].

Steps Involved in the Preparation of Alumina Sol-

$$Al(NO_3)_3.9H_2O + C_2H_5OH \xrightarrow{\text{Hydrolysis and condensation}} Al(OH)_3$$

$$2Al(OH)_3 \rightarrow Al_2O_3 + 3H_2O$$

Preparation of Zirconia Sol

The zirconia sol was prepared by precursor zirconium (IV) isopropoxide solution (70 wt% in 1 – propanol). The precursor solution was hydrolyzed by adding propanol solution to it with the help of a small amount of base (NH_4OH). 0.5 ml of zirconium (IV) isopropoxide was taken and this was diluted by using 50 ml propanol. 1 ml of ammonium hydroxide was added to catalyze the reaction. After continuous stirring for 3-4 hours at 110˚ C, the solution was kept for 4 days to complete the reaction. The nano zirconia sol was prepared and is ready for further characterization and use.

Steps Involved in the Preparation of Zirconia Sol-

$$Zr(C_3H_7)_4 + C_3H_7OH + NH_4OH \rightarrow Zr(OH)_4 + C_3H_7OH + NH_3$$

$$Zr(OH)_4 \xrightarrow{\text{Condensation}} [Zr(OH)_4]_n.xC_3H_7OH.xH_2O$$

Gel

$$[Zr(OH)_4]_n.xC_3H_7OH.xH_2O \xrightarrow{110^{\circ}C} n\,Zr(OH)_4 + xC_3H_7OH + x\,H_2O$$

Amorphous Gel

$$[Zr(OH)_4] + \text{Solvent} \xrightarrow{\text{Stirring}} ZrO_2$$

Zirconia sol

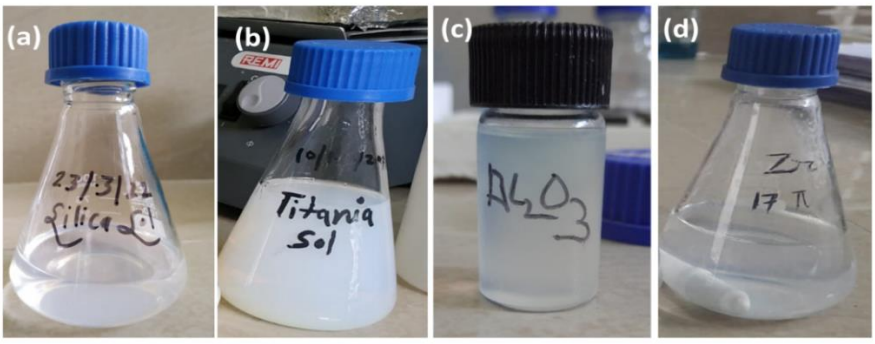

Figure 2. Images of prepared sol solutions: (a) Silica sol,(b) Titania sol,(c) Alumina Sol,(d) Zirconia Sol.

CHARACTERIZATION

Prepared silica sol, titania sol, alumina sol, and zirconia sol were characterized by the following analysis.

Tyndall Effect

This effect of light on moving colloidal particles, so that the path of moving particles is visible, is called the Tyndall effect. This phenomenon is observed when the wavelength of a light beam is comparable with the size of the particle; the light is scattered in such a way that the path of the colloidal particle is visible. Colloidal (nano-dimensional) particles show this effect. The laser light of 532 nm was passed through each solution as well as through the water solution. The difference between the water and colloidal particles in the presence of laser light is observed.

Particle Size Analysis (PSA), Zeta Potential, and Polydispersity Index (PDI)

To calculate the average size of particles in the sol solution of each sol, particle size distribution was analyzed. Zeta potential is the potential between the nanoparticle charge and a thin layer of charge over the surface. The magnitude of zeta potential defines its stability. To determine the stability and surface charge distribution of nanoparticles in the colloidal suspension, the zeta potential of the nanoparticles is observed. The polydispersity Index (PDI) shows the distribution of particles. If the value of PDI is high, the distribution is broad. So, only the average value of particle size (Z_{avg}) does not represent particle size satisfactorily. Along with the average value of particle size, PDI is also necessary. If the PDI value of nanoparticles is near zero, then it is monodispersed in nature, while if it goes towards 1, the polydispersity distribution range of particles increases. More polydispersity means a greater tendency for aggregation of particles than monodisperse. The particle size and zeta potential of sols were characterized by Instrument- Malvern 3000 Zetasizer Nano ZS (Malvern Instruments, Malvern, WR14 1XZ, UK), Graphic Era Deemed to be University, Dehradun.

Fourier Transform Infrared Spectroscopy (FTIR)

FTIR was used to characterize the prepared sols; its spectrum helps to analyze different functional groups, bonding structure, and organic groups present in the material. The principle behind IR spectroscopy is that the IR radiation passes through the material, and the sample responds according to its composition. Some phenomena like absorption, reflection, or transmittance occur in the sample. These changes are observed by the instrument, and it draws the IR spectrum of the sample. Every compound shows its unique IR spectrum, which is known as the molecular fingerprint region. The FTIR spectra of the prepared sols were analyzed by Perkin Elmer Spectrum II, Graphic Era Deemed to be University, Dehradun.

RESULTS AND DISCUSSION

Different sol solutions were prepared, such as Silica (SiO_2), Titania (TiO_2), Alumina (Al_2O_3), and Zirconia (ZrO_2). Images of prepared sol solutions are shown in the following Figure 2.

Tyndall Effect

Being nano-dimensional, prepared sol solutions should show the Tyndall effect. The behaviour of the laser light beam towards the sol solutions is shown in the following Figure 3.

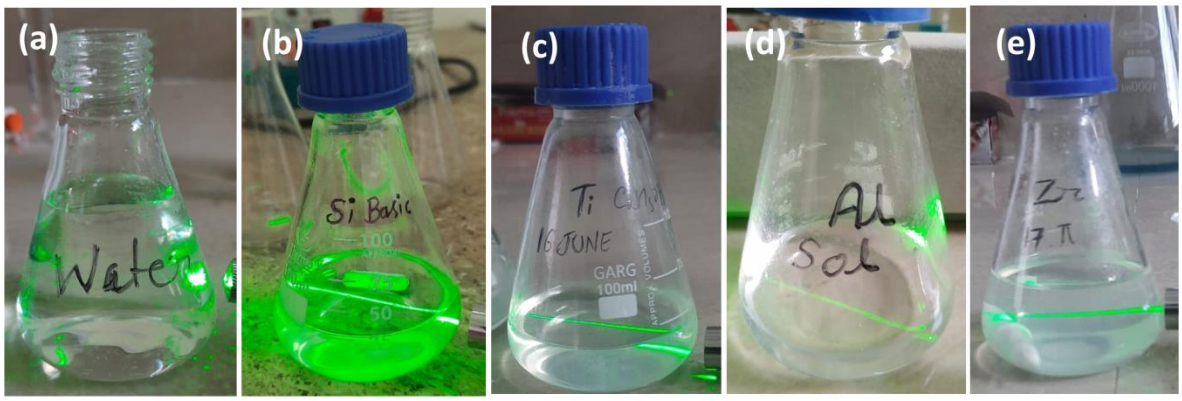

Figure 3. Effect of light beam on (a) water, (b) silica sol, (c) titania sol, (d) alumina sol, (e) zirconia sol.

Table. 1. Prepared sol solutions, their zeta potential, and poly-dispersity index.

Type of sol	Composition of sol	Avg Particle Size, Zavg (nm)	Zeta potential (mv)	Polydispersity index	Stability
Silica sol (base catalyzed)	Tetra ethoxy ortho silicate (TEOS)	78.88	-54.02	0.265	Highly stable
Silica sol (acid catalyzed)	Tetra ethoxy ortho silicate (TEOS)	102.5	-34.67	0.216	Highly stable
Titania sol	Titanium isopropoxide	119.6	-31.78	0.4545	Highly stable
Alumina sol	Aluminium iso propoxide	94.89	-49.56	0.378	Highly stable
Zirconia sol	Zirconium iso isopropoxide	86.43	-53.39	0.331	Highly stable

As it can be observed and differentiated between the effect of light on water and sol solutions. The path of light cannot be seen in the water solutions, as there is no presence of nanoparticles in the solutions. All sol solutions, because of the presence of nano-range colloidal particles, show a Tyndall effect when light passes through them. When the light of a specific wavelength encountered particles of nano range, which are continuously moving here and there in the solution (Brownian motion), the light got scattered, and it too scattered whenever it encountered with next particle in the path, because of this scattering of light the path of whole light is visible, and also small particles which are on the path also visible. This behaviour can be seen as a straight line of light in the case of all sol solutions (from Figure 3 b-e), while in the case of water no hindrance in the path of light, because no particles were present, so no light path is seen (Figure 3a). The Tyndall effect of light confirms that the particle ranges in the sol solutions are in the colloidal range [16].

Particle Size Analysis, Zeta Potential, and Polydispersity Index

The particle size of prepared sol solutions, their zeta potential, and polydispersity index are shown in the following Figure 4 and summarized in the Table. 1.

A nano range of various sols was confirmed by Particle size analysis. Zeta potential values for all prepared sols -54.02, -34.67, -31.78, -49.56, and -53.39 mV, respectively, for silica, titania, alumina, and zirconia sols, which specifies very high stability of all nano sol solutions. All the samples are not highly distributed because PDI values are 0.265, 0.216, 0.4545, 0.378, and 0.331 for silica, titania, alumina, and zirconia sols, respectively, which are much lower than 1. This shows the ranges of the particles are similar to the ranges in the solution. Not much variation in particle size was observed in the solution.

Fourier Transform Infrared Spectroscopy (FTIR)

Silica Nano- Sol IR Spectra

The IR spectra of silica sols by base-catalysis and acid-catalysis are shown in Figures 5 and 6, respectively.

In both of the prepared silica sol samples, broad peak appeared around 3300 cm^{-1} and 1650 cm^{-1}, these peaks were because of molecular water and –OH bonding vibrations. –C-H stretching of the solvent group appeared at 2974 cm^{-1}. The peak at 1925 cm^{-1} indicating the Si-H bonding. The stretching of the C-bond of the solvent molecule was confirmed by the peak at 1381 cm^{-1}. The band that appeared around 965 cm^{-1} represents the stretching vibrations of the free silanol (Si-O-Si) group present in the silica network of the sol solution. Peaks at 1047 cm^{-1} are stretching vibrations of Si-O-Si bonds. The IR absorption band at 882 cm^{-1} is due to vibrations of SiO_4. The band at 788 cm^{-1} is associated with the bending vibration of -C-H of the $-CH_3$-O-Si group [17-20].

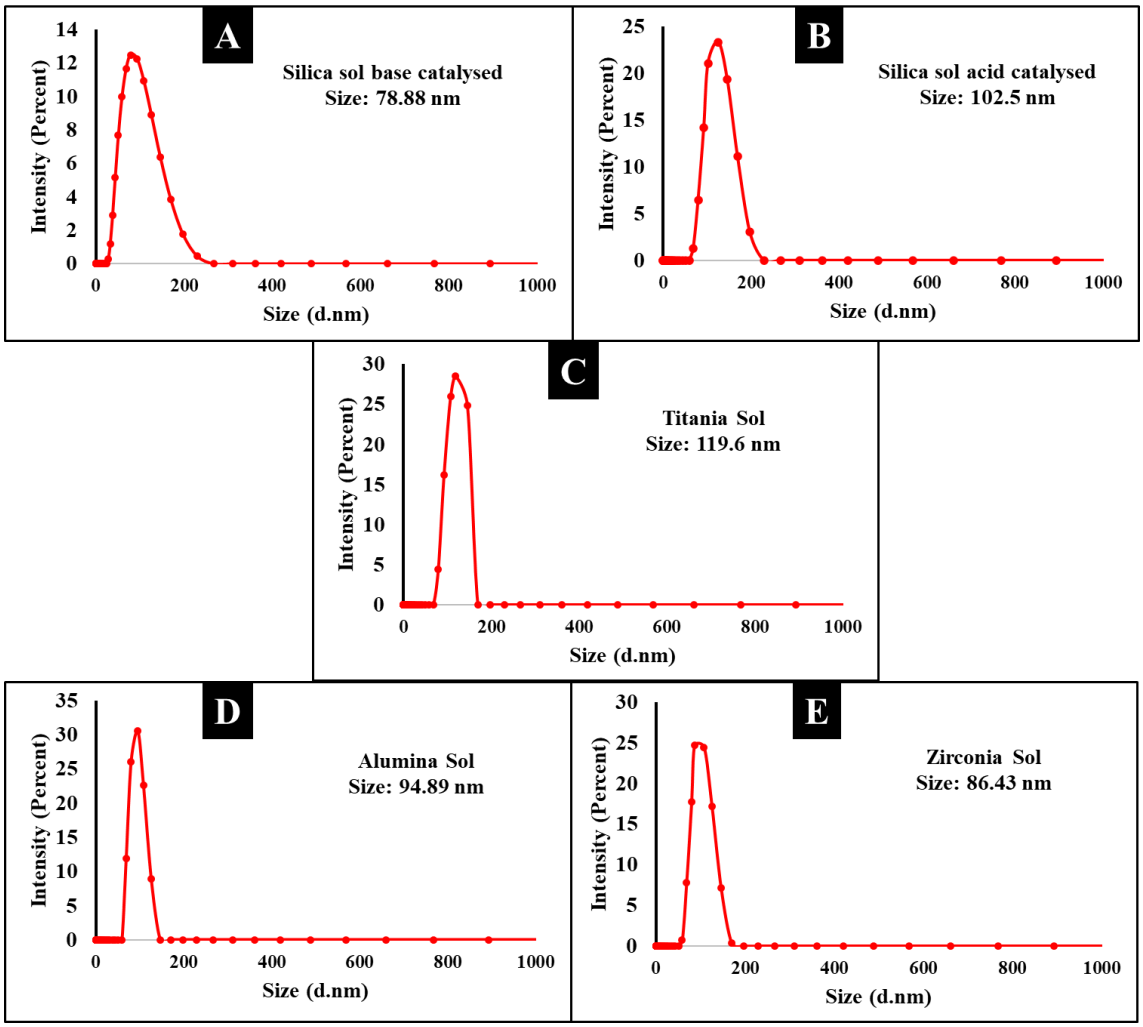

Figure 4. Particle size analysis results in a graphical manner with respect to intensity, (a) silica sol (base catalyzed), (b) silica sol (acid-catalyzed), (c) titania sol, (d) alumina sol (e) zirconia sol.

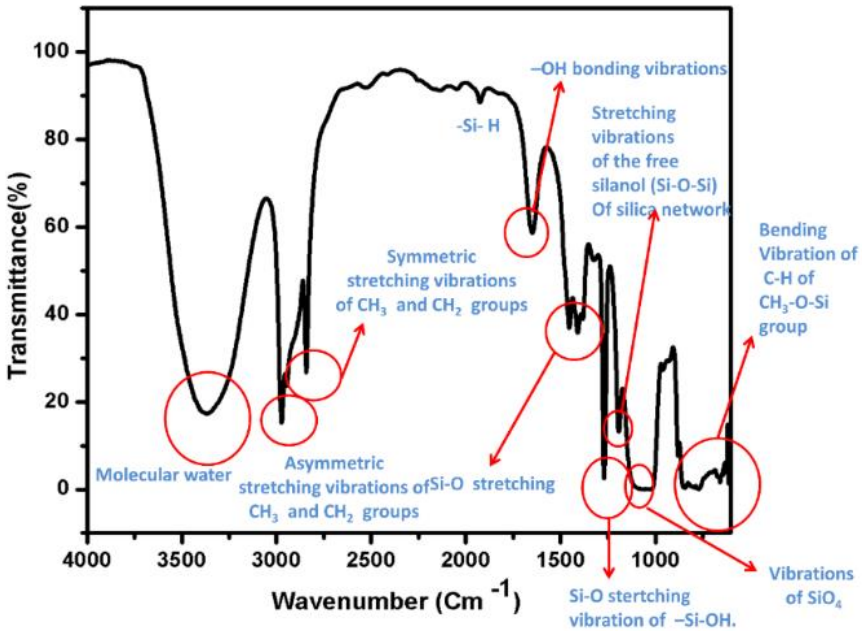

Figure 5. FTIR spectra of base-catalyzed silica sol.

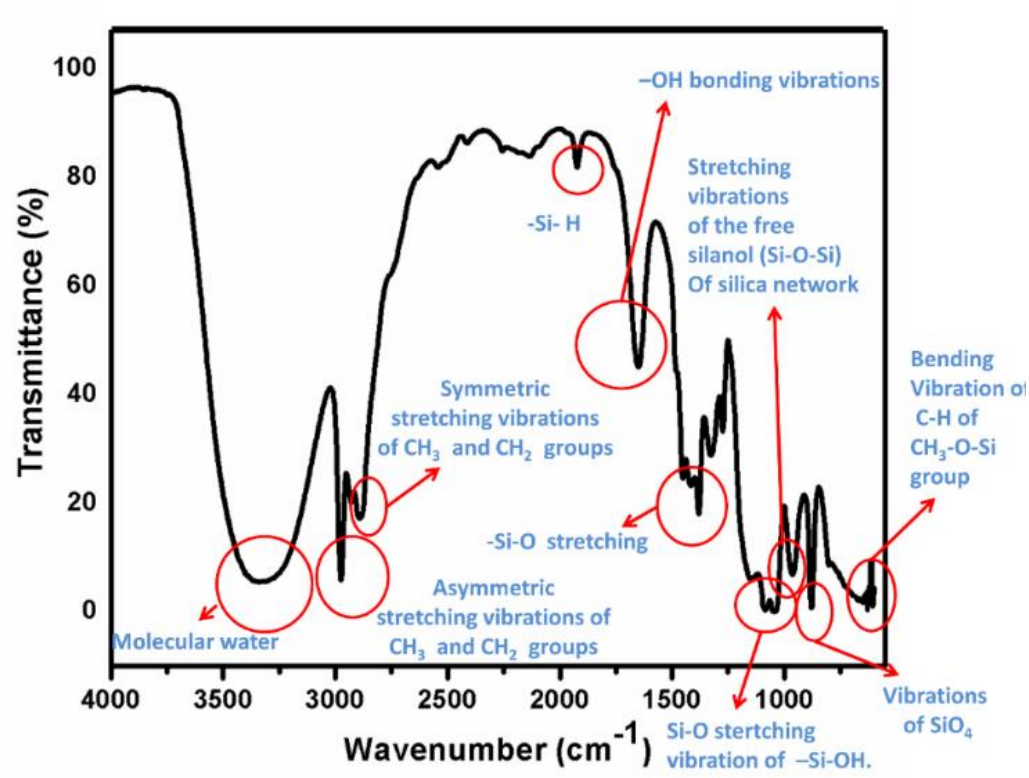

Figure 6. FTIR spectra of acid-catalyzed silica sol.

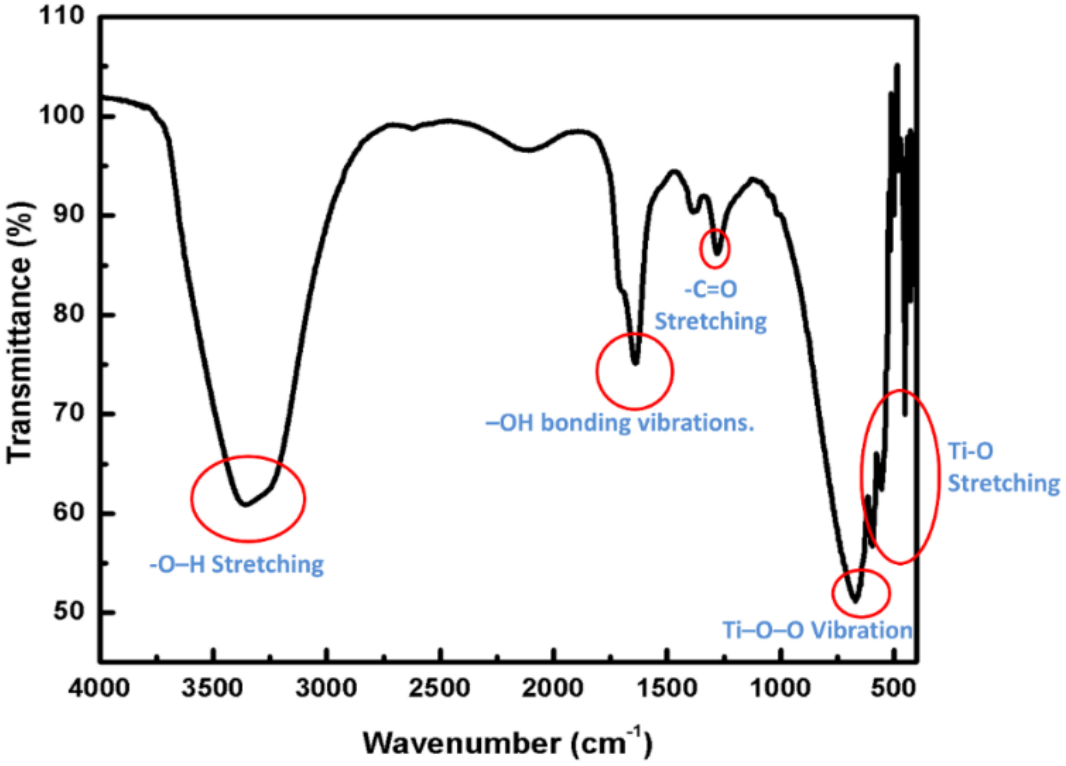

Figure 7. Titania nanoparticle IR spectra.

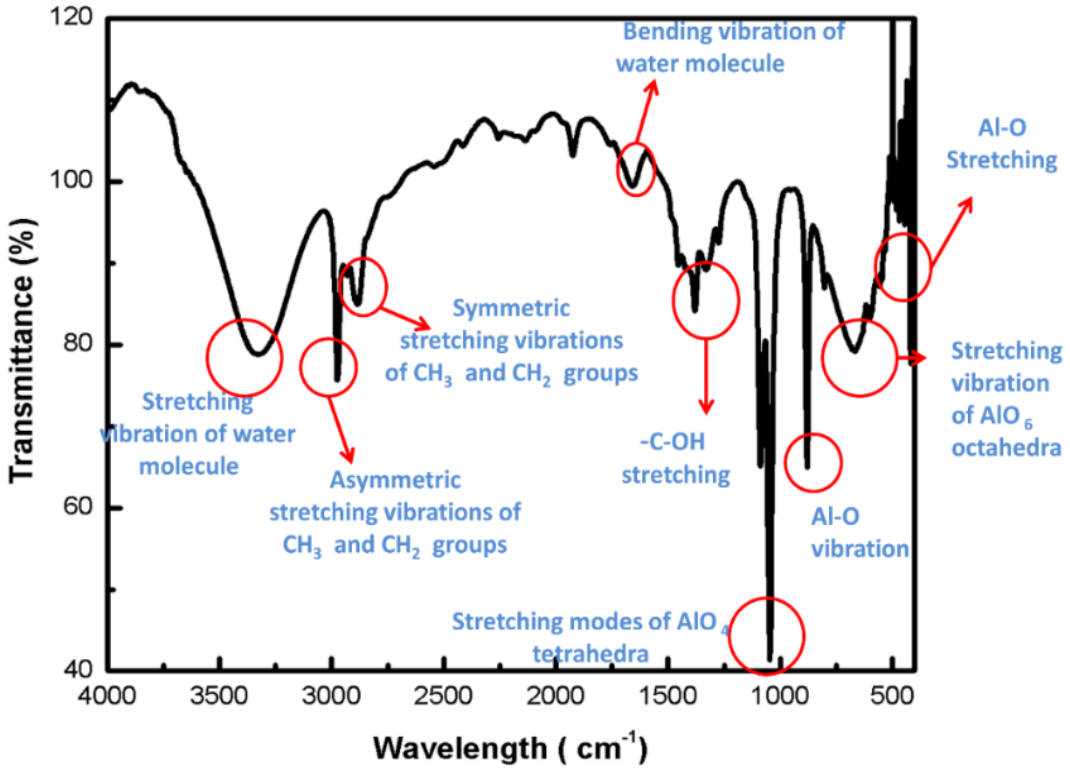

Figure 8. Alumina nanoparticle IR spectra.

Titania Nano Sol IR Analysis

In Figure 7, the FTIR spectrum of titania is shown. A broad peak appearing at 3353 cm^{-1} is the fundamental stretching vibration of O–H hydroxyl groups due to the presence of water molecules as solvent. Also, the sharp peak at 1638 cm^{-1} is because of the hydroxyl group (Bending vibration of the –O-H group). The peak arises at 1281 cm^{-1}, predicted by the –C=O stretching by the solvent molecule (As acetic acid was added for sol preparation). The vibration of the Ti-O-O peak was observed at 681 cm^{-1}. The peaks at 591 cm^{-1}, 527 cm^{-1}, and 452 cm^{-1} are assigned to the Ti–O stretching bands.

The observed peak was analyzed and compared with TiO_2 FTIR spectra. It shows the prepared sol contains TiO_2 nanoparticles [21-23].

Alumina Nanosol IR Spectra

Figure 8 represents the IR spectra observed by FTIR analysis of the prepared alumina sol solution.

The following peaks are seen clearly on the spectra. The first peak at 3353 cm^{-1} is due to the fundamental stretching vibration of -O–H hydroxyl groups. Peaks arise at 2900 cm^{-1} and 2884 cm^{-1} as a result of asymmetric stretching vibrations and symmetric stretching vibrations of CH_3 and CH_2 groups. These vibrations appear because of the presence of residues of the solvent molecule. A peak which is showing at 1659 cm^{-1} represents the bending vibration of the –O-H group. The peak at 1379 cm^{-1} also appeared because of the -C-OH stretching of the solvent molecule. Now, the peaks by alumina nanoparticles generally occur in the lower range of the IR spectrum. The IR spectrum shows the prepared alumina nanoparticles showing a spinel structure, where one Al atom is tetrahedral, and one Al atom is octahedrally coordinated. These two different peaks can be seen in the IR spectra. Stretching modes of tetrahedra appeared at 1046. Al-O vibrations occur at 881 cm^{-1} and 603 cm^{-1}. The 667 cm^{-1} peak represents the Stretching vibrations of octahedral sites of Al [24-27].

After comparing the spectra of the observed alumina nano sol, it is found that it is the spectra of γ-alumina nanoparticles sol.

Zirconia Nanosol IR Spectra

The observed IR spectrum of the prepared zirconia sol solution is shown in Figure 9.

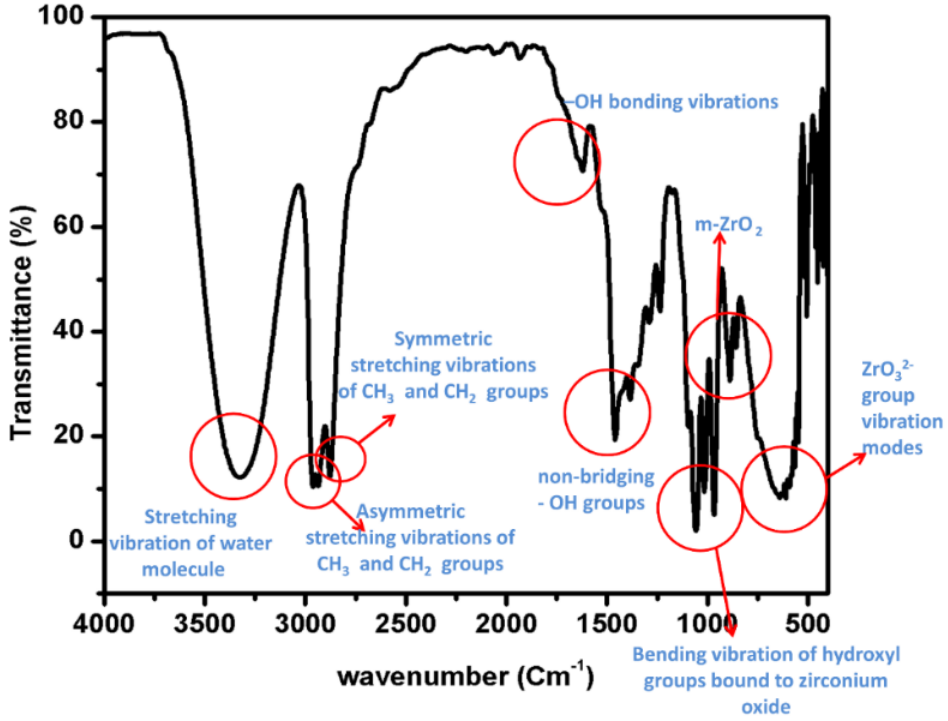

Figure 9. Zirconia nanoparticle IR spectra.

The IR spectra recorded from 400 to 4000 cm^{-1} for the prepared sol solution of zirconia. The bending vibrations of -OH groups of the water molecule and the stretching vibration of –OH groups of water molecules appear at 3000 cm^{-1} and 1,624.5 $cm^{-1,}$ respectively. The bending vibrations of hydroxyl groups, bound to zirconium oxide, were observed at 1,124.8 cm^{-1} and 800 cm^{-1} [28].

The peak observed at 1387 cm^{-1} represents the non-bridging OH groups being absorbed. The sharp peak at 735 cm^{-1} is characteristic of m-ZrO_2 (Monoclinic Zirconium Dioxide). The peak at 503 cm^{-1} is defined as the vibration mode of the ZrO_3^{2-} group in the prepared ZrO_2 sample, which shows the formation of ZrO_2 in the prepared sol solution [29].

CONLUSION

Silica (SiO_2) nano-sol, titania (TiO_2) nano-sol, alumina (Al_2O_3) nano-sol, and zirconia (ZrO_2) nano-sol were successfully prepared by sol-gel methodology. All prepared sols had a nano-dimensional particle range showing high stability in solution, which was confirmed by particle size analysis and zeta potential. Laser light was also used for determining the behaviour of particles, as colloidal particles show a Tyndall effect with laser light. The confirmation of the composition of nanoparticles was done by FTIR analysis. Prepared nano-sols can be further used for various applications of nanotechnology. Silica sol is showing a size of 78.88 nm when hydrolysis is done in basic condition by using NH_4OH, it generally leads to branched, highly cross-linked siloxane structures and the fast nucleation promotes the formation of many nuclie at once and also not agglomerated while on the other side, in acid catalysis promotes slower hydrolysis but showing slower nucleation results in fewer nuclie leading to grow them overtime into larger particle (102.5 nm). In titania sol, TTIP is highly reactive with water, even in the acid-hydrolysis, it undergoes rapid hydrolysis, especially at elevated temperatures (60°C), producing titanium hydroxide species. The hydrolysed particles tend to aggregate due to hydrogen bonding and van der Waals forces, forming a loose sol network. The large particle size (119.6 nm) is due to both fast nucleation and uncontrolled growth, coupled with particle fusion during ageing. The reaction between aluminium nitrate and NaOH leads to the formation of aluminium hydroxide, which then condenses into alumina nanoparticles. Despite stirring at 600 rpm, the room temperature limits the extent of reaction control, and NaOH promotes fast nucleation followed by secondary particle growth. The relatively large size (94.89 nm) indicates some degree of particle growth and aggregation, possibly due to electrostatic instability in ethanol. Also, nitrate byproducts can influence ionic strength, leading to less effective charge

stabilization and enhanced aggregation. Zirconium alkoxides are highly sensitive to hydrolysis, and at 110°C, rapid hydrolysis and condensation occur. The use of NH_4OH enhances nucleation, but at high temperature, both hydrolysis and condensation are accelerated, leading to particle growth and coalescence. The relatively smaller size (86.43 nm) compared to titania and alumina can be due to the lower initial precursor concentration and better miscibility of zirconium precursor in propanol, offering improved dispersion. High-temperature stirring also favours crystallite formation while limiting excessive particle growth.

DATA AVAILABILITY STATEMENT

The authors confirm that the data supporting the findings of this study are available within the article. Raw data that support the findings of this study are available from the corresponding author, upon reasonable request.

CREDIT AUTHORSHIP CONTRIBUTION STATEMENT

Neha Bhattt: Writing – original draft, Methodology. Adeeba Mirza: Writing – review & editing, Formal analysis, Investigation. Abhilasha Mishra: Writing – review & editing, Supervision, Conceptualization, Validation.

DECLARATION OF COMPETING INTEREST

The authors declare that they have no known competing financial interests or personal relationships that could have appeared to influence the work reported in this paper.

REFERENCES

1. Sonawane, L. D., Mandawade, A. S., Gite, A. B., Shinde, S. D., Patil, G. E., Nikam, L. K., ... & Shinde, M. S. (2025). Sol–gel synthesis of silicon oxide (SiO2) nanoparticles: exploring gas sensing and photocatalytic applications. Journal of Materials Science: Materials in Engineering, **20(1)**, 8. https://doi.org/10.1186/s40712-025-00209-8

2. Waghmode, M. S., Gunjal, A. B., Mulla, J. A., Patil, N. N. and Nawani, N. N. (2019) Studies on the titanium dioxide nanoparticles: Biosynthesis, applications and remediation. *SN Applied Sciences*, **1(4)**, 1–9. https://doi.org/10.1007/s42452-019-0337-3.

3. Piriyawong, V., Thongpool, V., Asanithi, P. and Limsuwan, P. (2012) Preparation and characterization of alumina nanoparticles in deionized water using laser ablation technique. *Journal of Nanomaterials*, **1**. https://doi.org/10.1155/2012/819403.

4. Sutha, S., Suresh, S., Raj, B. and Ravi, K. R. (2017) Transparent alumina based superhydrophobic self-cleaning coatings for solar cell cover glass applications. *Solar Energy Materials and Solar Cells*, **165**, 128–137. https://doi.org/10.1016/j.solmat.2017.02.027.

5. Jani, A. M. M., Losic, D. and Voelcker, N. H. (2013) Nanoporous anodic aluminium oxide: Advances in surface engineering and emerging applications. *Progress in Materials Science*, **58(5)**, 636–704. https://doi.org/10.1016/j.pmatsci. 2013.01.002.

6. Rogojan, R., Andronescu, E., Ghitulica, C. and Vasile, B. S. (2011) Synthesis and characterization of alumina nano-powder obtained by sol-gel method. *UPB Scientific Bulletin, Series B: Chemistry and Materials Science*, **73(2)**, 67–76.

7. Said, S., Mikhail, S. and Riad, M. (2020) Recent processes for the production of alumina nanoparticles. *Materials Science for Energy Technologies*, **3**, 344–363. https://doi.org/10.1016/ j.mset.2020.02.001.

8. Adak, D., Bhattacharyya, R. and Barshilia, H. C. (2022) A state-of-the-art review on the multi-functional self-cleaning nanostructured coatings for PV panels, CSP mirrors and related solar devices. *Renewable and Sustainable Energy Reviews*, **159**, 112145. https://doi.org/10.1016/ j.rser.2022.112145.

9. Wen, S. F., Wang, Y. M., Zhang, Z. M. and Liu, Y. L. (2019) Application of anti-icing coating based on adsorption of functional substances by microporous sphere. *Progress in Organic Coatings*, **137**, 105320. https://doi.org/10.1016/j.porgcoat.2019.105320.

10. Li, B., Liu, X., Zhang, X. and Chai, W. (2015) Stainless steel mesh coated with silica for oil–water separation. *European Polymer Journal*, **73**, 374–379. https://doi.org/10.1016/j.eurpolymj. 2015.10.031.

11. Liang, Y., Sun, S., Deng, T., Ding, H., Chen, W. and Chen, Y. (2018) The preparation of TiO_2 film by the sol-gel method and evaluation of its self-cleaning property. *Materials*, **11(3)**, 450. https://doi.org/10.3390/ma11030450.

12. Daoud, W. A. and Xin, J. H. (2004) Low temperature sol-gel processed photocatalytic titania coating. *Journal of Sol-Gel Science and Technology*, **29**, 25–29. https://doi.org/10.1023/B:JSST.0000016134.19752.b4.

13. Raji, Y. O., Othman, M. H. D., Nordin, N. A. H. S. M., Adam, M. R., Said, K. A. M., Ismail, A. F. and Alftessi, S. A. (2021) Synthesis and characterization of superoleophobic fumed alumina nanocomposite coated via the sol-gel

process onto ceramic-based hollow fibre membrane for oil-water separation. *Ceramics International*, **47(18)**, 25883–25894. https://doi.org/10.1016/j.ceramint.2021.05.319.

14. Pietrzyk, B., Miszczak, S., Kaczmarek, Ł. and Klich, M. (2018) Low friction nanocomposite aluminum oxide/MoS_2 coatings prepared by sol-gel method. *Ceramics International*, **44(7)**, 8534–8539. https://doi.org/10.1016/j.ceramint. 2018.02.055.

15. Hajizadeh-Oghaz, M., Shoja Razavi, R. and Ghasemi, A. (2015) Synthesis and characterization of ceria–yttria co-stabilized zirconia nanoparticles by sol–gel process for thermal barrier coatings applications. *Journal of Sol-Gel Science and Technology*, **74(3)**, 603–612. https://doi.org/10. 1007/s10971-015-3639-y.

16. Hassan, P. A., Rana, S. and Verma, G. (2015) Making sense of Brownian motion: colloid characterization by dynamic light scattering. *Langmuir*, **31(1)**, 3–12. https://doi.org/10.1021/ la501789z.

17. Protsak, I., Pakhlov, E., Tertykh, V., Le, Z. C. and Dong, W. (2018) A new route for preparation of hydrophobic silica nanoparticles using a mixture of poly (dimethylsiloxane) and diethyl carbonate. *Polymers*, **10(2)**, 116. https:// doi.org/10.3390/polym10020116.

18. Chen, X., Jiang, J., Yan, F., Tian, S. and Li, K. (2014) A novel low temperature vapor phase hydrolysis method for the production of nano-structured silica materials using silicon tetrachloride. *RSC Advances*, **4(17)**, 8703–8710. https://doi.org/10.1039/ C3RA47018K.

19. Kopani, M., Mikula, M., Takahashi, M., Rusnák, J. and Pinčík, E. (2013) FTIR spectroscopy of silicon oxide layers prepared with perchloric acid. *Applied Surface Science*, **269**, 106–109. https://doi.org/ 10.1016/j.apsusc.2012.09.081.

20. Chen, C., Jia, Z., Wang, X., Lu, H., Guan, Z. and Yang, C. (2015) Micro characterization and degradation mechanism of liquid silicone rubber used for external insulation. *IEEE Transactions on Dielectrics and Electrical Insulation*, **22(1)**, 313–321. https://doi.org/ 10.1109/TDEI.2014.004188.

21. Karkare, M. M. (2014) Choice of precursor not affecting the size of anatase TiO_2 nanoparticles but affecting morphology under broader view. *International Nano Letters*, **4(3)**, 1–8. https://doi. org/10.1007/s40089-014-0111-x.

22. Gohari, G., Mohammadi, A., Akbari, A., Panahirad, S., Dadpour, M. R., Fotopoulos, V. and Kimura, S. (2020) Titanium dioxide nanoparticles (TiO_2 NPs) promote growth and ameliorate salinity stress effects on essential oil profile and bio-chemical attributes of *Dracocephalum moldavica*. *Scientific Reports*, **10(1)**, 1–14. https://doi.org/ 10.1038/s41598-020-57794-1.

23. Praveen, P., Viruthagiri, G., Mugundan, S. and Shanmugam, N. (2014) Structural, optical and morphological analyses of pristine titanium dioxide nanoparticles synthesized via sol–gel route. *Spectrochimica Acta Part A*, **117**, 622–629. https://doi.org/10.1016/j.saa.2013.09.037.

24. Romero Toledo, R., Ruíz Santoyo, V., Moncada Sánchez, D. and Martínez Rosales, M. (2018) Effect of aluminum precursor on physicochemical properties of Al_2O_3 by hydrolysis/precipitation method. *Nova Scientia*, **10(20)**, 83–99. https://doi. org/ 10.21640/ns.v10i20.1217.

25. Vasconcelos, D. C., Nunes, E. H. and Vasconcelos, W. L. (2012) AES and FTIR characterization of sol–gel alumina films. *Journal of Non-Crystalline Solids*, **358(11)**, 1374–1379. https://doi.org/10. 1016/j.jnoncrysol.2012.03.017.

26. BN, V. H. and Sankaran, R. (2019) Performance of cutting tool with cross-chevron surface texture filled with green synthesized aluminium oxide nanoparticles. *Scientific Reports*, **9(1)**, 1–9. https:// doi.org/10.1038/ s41598-019-54346-0.

27. Manyasree, D., Kiranmayi, P. and Kumar, R. (2018) Synthesis, characterization and anti-bacterial activity of aluminium oxide nano-particles. *International Journal of Pharmacy and Pharmaceutical Sciences*, **10(1)**, 32–35. https://dx.doi.org/10.22159/ijpps.2018v10i1.20636.

28. Yakout, S. M. and Hassan, H. S. (2014) Adsorption characteristics of sol gel-derived zirconia for cesium ions from aqueous solutions. *Molecules*, **19(7)**, 9160–9172. https://doi.org/10.3390/ molecules19079160.

29. Rao, T. N., Hussain, I., Lee, J. E., Kumar, A. and Koo, B. H. (2019) Enhanced thermal properties of zirconia nanoparticles and chitosan-based intumescent flame retardant coatings. *Applied Sciences*, **9(17)**, 3464. https://doi.org/10.3390/app9173464.